International Journal of Current Research in Multidisciplinary (IJCRM) *ISSN: 2456-0979*
Vol. 5, No. 2, (February'20), pp. 21-27

DESCRIBED STRESS CONCENTRATION FACTORS OF AN INTERNALLY PRESSURIZED CYLINDER WITH HOLE BY NEW FORMULAS

Javad Jafari Fesharaki
[1]*Departmentof mechanical engineering, Najafabad Branch, Azad university, NajafAbad, Iran*

Abstract:
The purpose of this paper is to investigate the stress concentration factor(SCF) for an internally pressurized cylinder with hole and based on detailed three-dimensional elastic FE analysis, a new comprehensive set of formulas for SCFs are proposed. These stress concentration factors are presented and discussed as a function of the ratio of cylinder diameter to the thickness of cylinder and hole diameter. The first ratio "D/100t" is equal to 1, 1.25, 1.5, 1.75, 2, 2.5, 2.75, 3, 3.25 and 3.5 and the second ratio "D/10d", cylinder internal diameter to the hole diameter, varies from 0.6, 0.9, 1.2, 1.5, 1.8, 2, 2.3, 2.7,3.1 and 3.5. Results are also presented for SCF of longitudinal, circumferential and Von Mises stresses.

Keywords: *pressure vessel, stress concentration, finite element method, parameter identification*

INTRODUCTION

Pressure vessels are commonly used in diverse applications and normally have cross bore[1]or holes for fluid inlets, outlets and nozzles[2], [3]. There are many different connection in their outlets and nuzzles for instance nozzle-sphere connections are very common connections that use in industry [4].The pressure vessels sometimes that researchers are interested in studying about it is Materials that are used in pressure vessels for instance some modern materials like FGPM [5].These materials and other modern materials plays a key role in many new technology such as robotic [6], [7]. As per optimizing the size and dimensions of pressure vessels in this case the optimization method introduced in [8], [9] and [10]could be considered. Also, there are many researches that is conducted on energy resources that has been used in pressure vessels and they use some technique to optimize energy consumption[11]–[13]. The pressure vessels has been developed in harvesting energy field and some methods like electromagnetic energy technology has been used [14], [15]. Energy harvesting, is an innovative idea on which many researchers around the globe is currently working because it has the potential of solving the energy dilemma and increase the infrastructures' sustainability[16].Many methods has been used to analyse this stress concentration. In some study by using some FEM software like ABAQUS and ANSYS, researchers analyse stress and strain in many different process on materials.[17],[18]. All main codes and standards in pressure vessel field are stress based[19], [20] and they show a strong dependence of the cyclic life on the maximum stress range and slight changes in the stress ranges result in large change in the number of allowed cycles. Therefore in cyclic fatigue critical cases, good estimate of stress components ore of paramount importance. So a thorough understanding of hole geometries on the stress distributions and stress concentration factors, specially should be a design requirement. The ASME boiler and pressure vessel code does not required detailed stress analysis but only sets the wall thickness necessary to keep the basic stress below on allowable stress. Safety factors and design rules [21]are assumed to cater for the high localized stresses. Holes in the sidewalls of pressure vessels create stress concentrations that significantly decrease the ability of the wall to withstand cyclic loading. These stress concentrations are considered "peak" stresses and are primarily considered when calculating the fatigue life of a vessel. According to points mentioned above, FEM is an appropriate method to analysis of stress and force[22]. In this paper by usage of FE analysis three comprehensive formulas for longitudinal, circumferential and Von Mises SCFs ore proposed. These formulas are presented as a function of the ratio of the cylinder internal diameter to the thickness of cylinder D/100t, and hole's diameter D/10d.

FINITE ELEMENT MODELLING AND GEOMETRY

2.1. Geometry

Fig. 1 shows sketch and notation of the cylindrical vessel with hole.

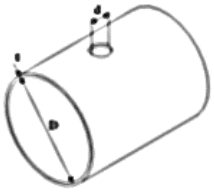

Figure1. Geometry and notation of cylindrical vessel with hole

The main cylinder has a mean diameter, D, thickness, t, and hole diameter, D. The ranges of geometry parameters included in this study are shown in table 1.

Table 1.Range of geometrical parameters

D/100t	**1**	**1.25**	**1.5**	**1.75**	**2**	**2.5**	**2.75**	**3**	**3.25**	**3.5**
D/10d	**0.6**	**0.9**	**1.2**	**1.5**	**1.8**	**2**	**2.3**	**2.7**	**3.1**	**3.5**

The constitutive law used was homogeneous, isotropic and linear elastic. The pressure, P, was considered to act on the inner surface of the cylinder. The material properties used I the FE analysis were: E= 2.07x105 MPa and a Poisson's ratio of 0.3, as employed in Ref.[3], was used throughout the calculation in order to be able to make a complete comparison with the results reported therein, including and especially the particular comparison for the so called SCF formula as proposed in this work.

2.2. FE Analysis

In this study the software used was ANSYS and as the maximum stress around the hole region should be measured from the FE analysis, the number of elements around it would be an important parameter. So regions around hole use relatively refined meshing. This mesh is believed to accurately represent the geometry, being minimal without losing information [23]. In this work the internal pressure is fixed and used in every case. As shown in table 1, a wide range of thickness and hole diameter ratios were analysed and the maximum longitudinal, circumferential and Von Mises stresses around hole can be easily determined from elastic FE analyses, from which the stress concentration factors can be determined by using the following expressions relatively:

$$K_t(longitudinal) = K_{tl} = \frac{\sigma_{\max\,(l)}}{\sigma_{nom}\,(l)} (1)$$

$$K_t(circumferential) = K_{tc} = \frac{\sigma_{max}\,(c)}{\sigma_{nom}\,(c)} (2)$$

$$K_t(vonmises) = K_{tv} = \frac{\sigma_{max}\,(v)}{\sigma_{nom}\,(v)} (3)$$

RESULT AND DISCUSSION

3.1. Results and formulas for SCFs

The calculation to determine the SCFs for the case treated in this analysis were performed by computing the maximum stress indicated in equations 1, 2 and 3. Fig. 2-7 shows the significant influence of D/100t and D/10d on the magnitude of the SCFs. As expected, the values of SCFs increase with increasing D/100t ratios and decrease with increasing D/10d. Also as shown in figures, the D/100t ratio has linear influence on SCFs, but the D/10d ratio has nonlinear influence on there and

the SCFs are more sensitive on D/10d in little values. The equations for the longitudinal, circumferential and Von-Mises SCFs in cylinders were developed as a function of D/100t and D/10d by curve fitting the finite element analysis results. These equations are given by the following, respectively:

$$K_{tl}\&K_{tc}\&K_{tv} = A\left(\frac{D}{10d}\right)^2 + B\left(\frac{D}{10d}\right) + C(4)$$

That for longitudinal SCF the parameters A, B and C are defined as:

$$A = 0.01\left(\frac{D}{100t}\right)^2 + 0.8\left(\frac{D}{100t}\right) + 0.4 \quad (5)$$

$$B = 0.044\left(\frac{D}{100t}\right)^2 - 0.2\left(\frac{D}{100t}\right) - 1.29 \quad (6)$$

$$C = -0.016\left(\frac{D}{100t}\right)^2 + 0.019\left(\frac{D}{100t}\right) + 1.03 \quad (7)$$

And for circumferential SCF, the parameters A, B and C are described as:

$$A = -0.095\left(\frac{D}{100t}\right)^2 + 2.38\left(\frac{D}{100t}\right) + 0.6 \quad (8)$$

$$B = -0.02\left(\frac{D}{100t}\right)^2 + 0.197\left(\frac{D}{100t}\right) - 1.56 \quad (9)$$

$$C = 0.008\left(\frac{D}{100t}\right)^2 - 0.35\left(\frac{D}{100t}\right) + 3.26 \quad (10)$$

And for von-mises SCF, the parameters A, B and C are determined as:

$$A = -0.108\left(\frac{D}{100t}\right)^2 + 2.74\left(\frac{D}{100t}\right) + 0.66 \quad (11)$$

$$B = -0.0216\left(\frac{D}{100t}\right)^2 + 0.206\left(\frac{D}{100t}\right) - 1.58 \quad (12)$$

$$C = 0.009\left(\frac{D}{100t}\right)^2 - 0.4\left(\frac{D}{100t}\right) + 3.78 \quad (13)$$

These equations were designed to be used in lieu of the graphs and charts to easily compute the stress concentration factors

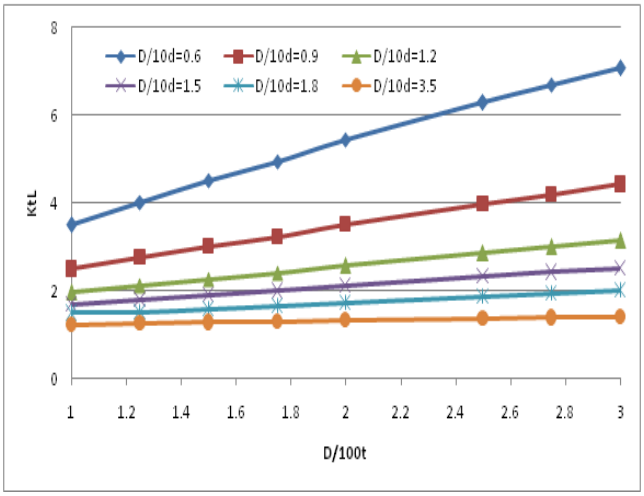

Figure 2. Longitudinal stress concentration factors with various ratio of D/10d

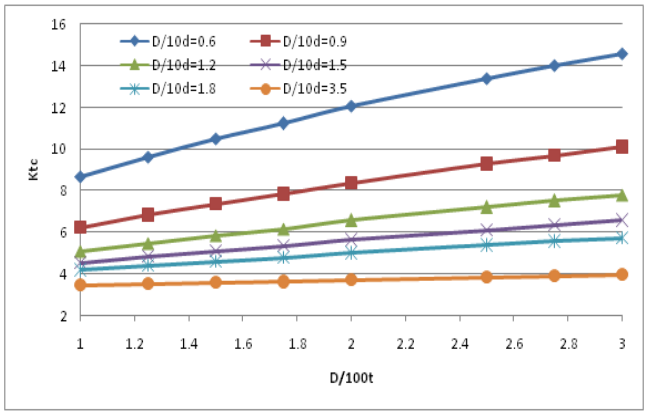

Figure3.Circumferential stress concentration factors with various ratio of D/10d

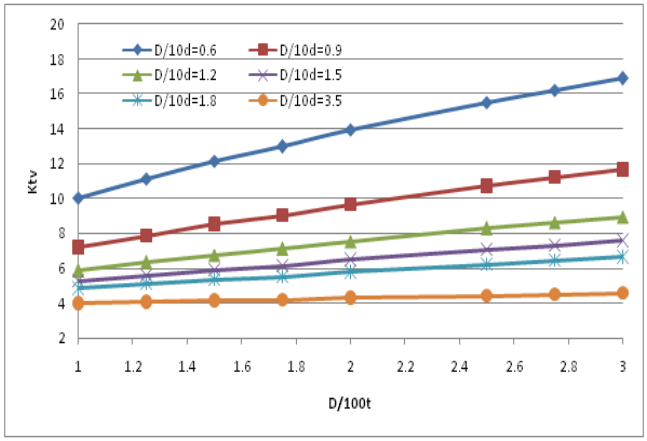

Figure 4. Von-Mises stress concentration factors with various ratio of D/10d

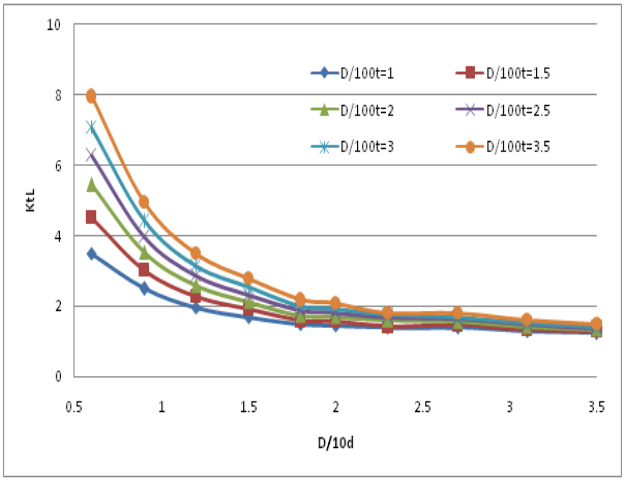

Figure 4. Longitudinal stress concentration factors with various ratio of D/100t

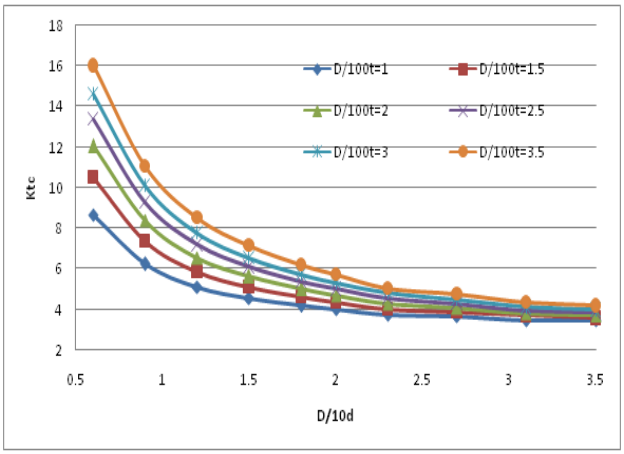

Figure 6. Circumferential stress concentration factors with various ratio of D/100t

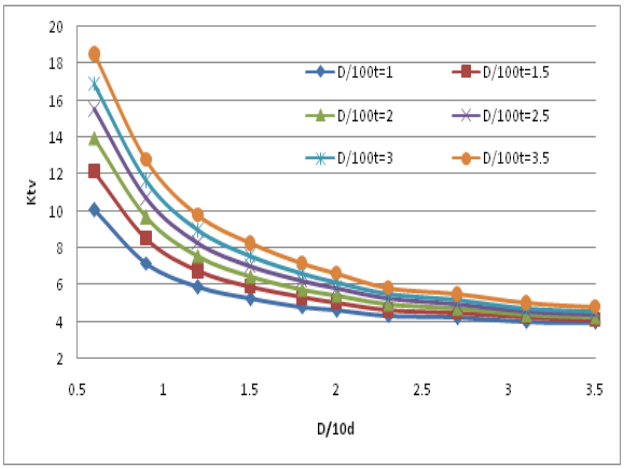

Figure 7. Von-Mises stress concentration factors with various ratio of D/100t

3.2. Checking the validity of the proposing equation to existing literature

Table 2 shows a comparison of the longitudinal stress concentration factors around hole in pressurized cylinder vessel in three different cases. Our analysis results are in good agreement with the experimental analysis in existing literature [24]. The errors between the results obtained from formulas and experimental tests are about max. 9.8%.

Table2. Longitudinal stress concentration factor around the hole in three cases

	D	D	T	D/100t	D/10d	KtL (test)	KtL (formula)	Error
1	1000	125	4.08	2.45	0.8	4.8	4.37	9.8%
2	1000	167	2.86	3.5	0.59	7.2	7.87	8.5%
3	1000	142.8	3.23	3.1	0.7	6.4	5.99	6.8%

CONCLUSION

In this work based on detailed 3D elastic F.E. analysis a new comprehension set of formulas for SCFs in an internally pressurized cylinder with hole are proposed. The results from these comprehensive formulas with the experimental results in existing literature are compared. Charts and formulas were developed as a function of the cylinder diameter to thickness of cylinder (D/100t) and hole diameter (D/10d). We recommend the following:

I. Insert the hole stress concentration factors chart and formulas presented in this paper in the ASME code, sec. VIII Div.3 so that they are readily accessible for their use in fatigue strength evaluation in pressurized cylinder.
II. Investigate the longitudinal, circumferential and von-mises stress distribution in plastic range around the hole in pressurized cylinder.
III. Investigate the effects and formulas for pressurized cylinder with elliptical hole and other kind of discontinuity.

REFERENCES

[1] R. D. Dixon, D. T. Peters, and J. G. M. Keltjens, "Stress Concentration Factors of Cross-Bores in Thick Walled Cylinders and Blocks," *J. Press. Vessel Technol.*, vol. 126, no. 2, pp. 184–187, May 2004, doi: 10.1115/1.1687381.

[2] H. F. Wang, Z. F. Sang, L. P. Xue, and G. E. O. Widera, "Elastic Stresses of Pressurized Cylinders With Hillside Nozzle," *J. Press. Vessel Technol.*, vol. 128, no. 4, pp. 625–631, Nov. 2006, doi: 10.1115/1.2349576.

[3] Y.-H. Liu, B.-S. Zhang, M.-D. Xue, and Y.-Q. Liu, "Limit pressure and design criterion of cylindrical pressure vessels with nozzles," *Int. J. Press. Vessels Pip.*, vol. 81, no. 7, pp. 619–624, Jul. 2004, doi: 10.1016/j.ijpvp.2004.04.002.

[4] S. Schindler and J. L. Zeman, "Stress concentration factors of nozzle-sphere connections," *Int. J. Press. Vessels Pip.*, vol. 80, no. 2, pp. 87–95, 2003, doi: 10.1016/S0308-0161(03)00026-7.

[5] R. Rashidifar, J. Jafari, H. Shahriary, and V. Jafari, "Analysis of FGPM cylinder subjected to two dimensional electro thermo mechanical fields," *Modares Mech. Eng.*, vol. 14, no. 4, pp. 83–90, Jul. 2014.

[6] N. Ebrahimi, "Simulation of a Three link- Six Musculo Skeletal Arm Activated by Hill Muscle Model," Aug. 2019, doi: 10.31224/osf.io/ckuh8.

[7] N. Ebrahimi, G. Muthukumaran, and A. Jafari, "Reduction in The Metabolic Cost of Human Walking Gaits Using Quasi-Passive Upper Body Exoskeleton," in *2019 International Symposium on Medical Robotics (ISMR)*, 2019, pp. 1–7, doi: 10.1109/ISMR.2019.8710200.

[8] N. Ebrahimi, P. Schimpf, and A. Jafari, "Design optimization of a solenoid-based electromagnetic soft actuator with permanent magnet core," *Sens. Actuators Phys.*, vol. 284, pp. 276–285, Dec. 2018, doi: 10.1016/j.sna.2018.10.026.

[9] N. Ebrahimi, S. Nugroho, A. F. Taha, N. Gatsis, W. Gao, and A. Jafari, "Dynamic Actuator Selection and Robust State-Feedback Control of Networked Soft Actuators," *2018 IEEE Int. Conf. Robot. Autom. ICRA*, pp. 2857–2864, 2018, doi: 10.1109/ICRA.2018.8460679.

[10] A. Jafari and N. Ebrahimi, "Electromagnetic soft actuators," US20200003088A1, 02-Jan-2020.

[11] M. Khatibi and S. Ahmed, "Optimal resilient defense strategy against false data injection attacks on power system state estimation," in *2018 IEEE Power Energy Society Innovative Smart Grid Technologies Conference (ISGT)*, 2018, pp. 1–5, doi: 10.1109/ISGT.2018.8403330.

[12] M. Khatibi and S. Ahmed, "Impact of Distributed Energy Resources on Frequency Regulation of the Bulk Power System," *ArXiv190609295 Cs Eess*, Jun. 2019.

[13] M. Khatibi , T. Amraee , H. Zargarzadeh ; M. Barzegaran "Comparative analysis of dynamic model reduction with application in power systems - IEEE Conference Publication." [Online]. Available: https://ieeexplore.ieee.org/abstract/document/7462823. [Accessed: 30-Jan-2020].

[14] M. Gholikhani, M. Sharzehee, S. A. Tahami, F. Martinez, S. Dessouky, and L. F. Walubita, "Effect of electromagnetic energy harvesting technology on safety and low power generation in sustainable transportation: a feasibility study," *Int. J. Sustain. Eng.*, vol. 0, no. 0, pp. 1–14, Nov. 2019, doi: 10.1080/19397038.2019.1688890.

[15] M. Gholikhani, S. A. Tahami, and S. Dessouky, "Harvesting Energy from Pavement – Electromagnetic Approach," *MATEC Web Conf.*, vol. 271, p. 06001, 2019, doi: 10.1051/matecconf/201927106001.

[16] M. Gholikhani, H. Roshani, S. Dessouky, and A. T. Papagiannakis, "A critical review of roadway energy harvesting technologies," *Appl. Energy*, vol. 261, p. 114388, Mar. 2020, doi: 10.1016/j.apenergy.2019.114388.

[17] R. Rashidifar, N. Ebrahimi, and M. Salem, "Finite Element Simulation of Rotary Forging Process for Manufacturing of Spur Gear and its Investigation in order to Predict Forces Acting on Mold,"

presented at the the Second National Conference of Mechanical Systems and industrial innovations, Ahvaz, Iran, 2014.

[18] R. Rashidifar, M. Khataei, M. Poursina, and N. Ebrahimi, "Comparison and Evaluation of Criteria Ductile Damage FLD & MSFLD to Predict Crack Growth in Forming Processes," presented at the the National Conference on Mechanical Engineering of Iran, Shiraz, Iran, 2014.

[19] "ASME Boiler and Pressure Vessel Code, Section VIII Division 2- Alternative rules for the construction of pressure vessels. New York: ASME; 1999." .

[20] "PD 5500:2000 Specification for unfired fusion welded pressure vessels (AMD 10830) (AMD 11002) (AMD Corrigendum 12088) (AMD 13241) (AMD Corrigendum 13558) (AMD Corrigendum 13707) (AMD 13879), British Standards Institution - Publication Index | NBS." .

[21] J. H. Faupel, "Pressure Vessels of Noncircular Cross Section (Commentary on New Rules for ASME Code)," *J. Press. Vessel Technol.*, vol. 101, no. 3, pp. 255–267, Aug. 1979.

[22] R. Rashidifar, P. Foude, and M. Poursina, "Finite Element Simulation of Cold Rolling Process and Calculation of Rolling Force Using Artificial Neural Network," presented at the the Twelfth National Conference of Iran Manufacturing Engineering, Iranian Society of Manufacturing Engineering, College of Engineering, Tehran, Iran, 2012.

[23] C. R. ALAVALA, *FINITE ELEMENT METHODS: Basic Concepts and Applications*. PHI Learning Pvt. Ltd., 2008.

[24] K. M. Marshek, "Stress concentration factors: R.E. Peterson: John Wiley & Sons, New York 1974, xiv + 317pp," 1975, doi: 10.1016/0094-114X(75)90065-8.

